

## Dynamics and Control of a Quadrotor Aircraft

S.A. Kava<sup>1</sup>

Department of Mechanical Engineering,  
Curtin University, Perth, Western Australia, 6102, Australia

### Abstract

During flight a quadrotor, vertical take-off and landing aircraft (VTOL), experiences aerodynamic loads (forces and moments). These loads are induced by airflow about the structure of the quadrotor and consist of both laminar and turbulent airflow. Despite this fact, all existing works on controlling quadrotors either ignore these loads, or only consider loads resulting from laminar airflow. This simplification or ignorance of the aircrafts dynamics deteriorates the quadrotor's control performance in a practical implementation. To address the difficulties associated with laminar and turbulent airflow during flight, the resulting aerodynamic loads are treated as deterministic and stochastic components respectively. This paper presents an extended model for a quadrotor which takes into account aerodynamic loading during flight using Newtonian and Lagrangian mechanics. Furthermore, a combination of Euler angles and Modified Rodrigues Parameters (MRP) are used for the attitude representation of the aircraft. This is to reduce the occurrence of singularities in the dynamic equations. A combined one-step ahead backstepping and standard backstepping controller is designed to achieve path-tracking control of the quadrotor. This control method is used to compare and contrast the effects of taking into account turbulent loads with ignoring these loads on the behavior of the quadrotor. Weak and strong nonlinear Lyapunov functions are used to overcome difficulties caused by underactuation and Hessian terms induced by the stochastic differentiation rule.

**Themes:** Aerodynamics, Turbulence.

### Introduction

Many engineering systems operate in the presence of adverse aerodynamic loads, including: aircraft frames, propeller blades, and any form of turbomachinery. In the past decade there has been growing interest in the use of Unmanned Aerial Vehicle (UAV), for both government and commercial applications. One problem with small UAVs such as quadrotors is their susceptibility to wind fields and gusts. These disturbances not only degrade the performance of the aircraft but can increase the danger of operating them in populated areas. When considering these aerodynamic disturbances a particular concern is turbulent airflow. Turbulent airflow with its chaotic nature can lead to drastic reductions in performance and at worst catastrophic failure and damage to property and personnel. However one of the many attractive attributes of the quadrotor is its simplistic structure, having a rigid cross frame body equipped with four fixed pitch propellers (see Figure 1). Due to the simplistic structure, the quadrotor has very poor aerodynamic properties. The quadrotors structure causes flow separation about the aircraft during flight to occur, exacerbating the effects of turbulence and increasing the aircrafts instability. The four rotors are configured such that two rotors counter-rotate relative to the other two. (i.e. two rotors turn clockwise and the other two counter-clockwise). The paired opposing rotation compensates for the reactive



Figure 1: Quadrotor helicopter.

torques that would cause the aircraft to yaw in an uncontrolled manner. The vertical motion (altitude) is obtained by the collective speed increase or decrease of all four rotors. The pitch and roll motion are obtained by changing the speed of the front-rear pair and the left-right pair of rotors, respectively. Yaw motion is realised by the difference in the reactive torques between the two pairs of counter rotating rotors. Horizontal motion (latitude and longitude) result from the combination of the pitch, roll and vertical motions. The motions of the quadrotor aircraft are nonlinearly coupled which increases the difficulty of controlling the aircraft. Furthermore, the aircraft is underactuated because there are only four independent control inputs, a pitching, a rolling and a yawing moments and a collective thrust. This is because each motor is fixed in position with only its rotor able to rotate, while the direction of thrust relative to the aircraft frame can not change. However, there are six degrees of freedom (latitude, longitude, altitude, pitch, roll, yaw) to be controlled, see [1] for more details on controlling other underactuated mechanical systems. Difficulties in controlling the motions of the quadrotor aircraft arise from the mentioned nonlinear coupling and underactuation. In addition the non-deterministic (chaotic) nature of turbulent airflow being applied to the airframe increases control difficulty. A brief review of the related works on controlling multi-rotor aircraft is given below to motivate contributions of the paper.

Because the quadrotor aircraft operates in three-dimensional (3D) space, controlling and examining the behaviour of all six degrees of freedom in flight has recently attracted attention of researchers in the control and robotics communities. Firstly, attitude control was obtained in [2] and [3], local position control in [4], [5] and [6]. Position control has also been addressed in [7] and [8]. Local position control was achieved on a physical quadrotor in [9], [10], [11] and [12]. However, a one-step ahead backstepping controller and the unit quaternion were used in [13] to obtain global asymptotic control. In all these works on control of quadrotor aircraft and others not listed here, the loads (forces and moments) induced by airflow on the aircraft were neglected or assumed to be deterministic. In practice these assumptions do not

hold, as wind loads acting on the aircraft always contain both laminar and turbulent flow. This paper treats these loads as having both deterministic and stochastic components respectively. In the case of the quadrotor, whose body is in no manner aerodynamic, neglecting these components can result in significant deterioration of control performance. As such, stochastic differential equations (SDE) will be used to model the dynamics of the aircraft. SDE's are useful for modelling systems, with high degrees of uncertainty which is not reasonable to be ignored. Such a situation is the case of turbulent airflow about an object.

## Aircraft Dynamics Modelling

For modelling the motion of the quadrotor Newtonian and Lagrangian mechanics are used instead of Navier–Stokes. This is because the later is significantly more difficult to design an in flight control scheme for. Thus, the equations of motion of a quadrotor are described by:

$$\dot{\boldsymbol{\eta}}_1 = \mathbf{v}_1, \quad (1)$$

$$\mathbf{v}_1 = \mathbf{R}_1(\mathbf{q})\mathbf{v}^b, \quad (2)$$

$$\dot{\mathbf{q}} = \mathbf{R}_2(\mathbf{q})\boldsymbol{\omega}, \quad (3)$$

$$\dot{\boldsymbol{\zeta}} = \mathbf{M}_b^{-1} \left( -\mathbf{D}\boldsymbol{\zeta} - \mathbf{C}_b(\boldsymbol{\zeta})\boldsymbol{\zeta} - \mathbf{G}_1(\mathbf{q}) + \begin{bmatrix} \mathbf{f}^b \\ \boldsymbol{\tau} \end{bmatrix} + \begin{bmatrix} \mathbf{f}_{Aero}^b \\ \boldsymbol{\tau}_{Aero} \end{bmatrix} \right), \quad (4)$$

where the position of the quadrotor's centre of mass is given by the vector  $\boldsymbol{\eta}_1 = [x \ y \ z]^T$  denoting the (latitude, longitude, altitude) displacements of the centre of mass of the aircraft coordinated in the earth-fixed frame. The vector  $\mathbf{v}_1 = [u \ v \ w]^T$  denotes the linear velocities of the aircraft coordinated in the earth-fixed frame. The vector  $\mathbf{v}^b$  denotes the linear velocities of the aircraft coordinated in the body fixed frame. The MRP  $\mathbf{q}$ , which represents the attitude (orientation) of the aircraft coordinated in the earth-fixed frame. The vector  $\boldsymbol{\omega}$  denotes the aircraft's angular velocity vector coordinated in the body-fixed frame. The vectors  $\mathbf{f}^b$  and  $\boldsymbol{\tau}$  represent the control forces and torques coordinated in the body-fixed frame. The vectors  $\mathbf{f}_{Aero}^b$  and  $\boldsymbol{\tau}_{Aero}$  represent the disturbance forces and torques coordinated in the body-fixed frame. The matrices  $\mathbf{R}_1(\mathbf{q})$  and  $\mathbf{R}_2(\mathbf{q})$  are given by:

$$\mathbf{R}_1(\mathbf{q}) = \mathbf{I}_{3 \times 3} + \frac{8\mathbf{S}(\mathbf{q})}{(1 + \|\mathbf{q}\|^2)^2} \left( \mathbf{S}(\mathbf{q}) - \frac{1 - \|\mathbf{q}\|^2}{2} \mathbf{I}_{3 \times 3} \right), \quad (5)$$

$$\mathbf{R}_2(\mathbf{q}) = \frac{1}{2} \left( \mathbf{q}\mathbf{q}^T + \mathbf{S}(\mathbf{q}) \frac{1 - \|\mathbf{q}\|^2}{2} \mathbf{I}_{3 \times 3} \right), \quad (6)$$

$$\mathbf{q} = \frac{1}{q_0} \begin{bmatrix} \sin\left(\frac{\phi}{2}\right)\cos\left(\frac{\theta}{2}\right)\cos\left(\frac{\psi}{2}\right) - \cos\left(\frac{\phi}{2}\right)\sin\left(\frac{\theta}{2}\right)\sin\left(\frac{\psi}{2}\right) \\ \cos\left(\frac{\phi}{2}\right)\sin\left(\frac{\theta}{2}\right)\cos\left(\frac{\psi}{2}\right) + \sin\left(\frac{\phi}{2}\right)\cos\left(\frac{\theta}{2}\right)\sin\left(\frac{\psi}{2}\right) \\ \cos\left(\frac{\phi}{2}\right)\cos\left(\frac{\theta}{2}\right)\sin\left(\frac{\psi}{2}\right) - \sin\left(\frac{\phi}{2}\right)\sin\left(\frac{\theta}{2}\right)\cos\left(\frac{\psi}{2}\right) \end{bmatrix},$$

$$q_0 = 1 + \cos\left(\frac{\phi}{2}\right)\cos\left(\frac{\theta}{2}\right)\cos\left(\frac{\psi}{2}\right) + \sin\left(\frac{\phi}{2}\right)\sin\left(\frac{\theta}{2}\right)\sin\left(\frac{\psi}{2}\right), \quad (7)$$

where  $\mathbf{I}_{3 \times 3}$  is a  $3 \times 3$  identity matrix.  $\mathbf{S}(\mathbf{x})$  is the skew-symmetric matrix of the vector  $\mathbf{x} = \text{col}(x_1, x_2, x_3) \in \mathbb{R}^3$  and  $\phi$ ,  $\theta$ , and  $\psi$  represent Euler angles defining the quadrotors attitude.

Moreover, we define:

$$\boldsymbol{\zeta} = \begin{bmatrix} \mathbf{v}^b \\ \boldsymbol{\omega} \end{bmatrix}, \quad \mathbf{M}_b = \begin{bmatrix} m & \mathbf{0}_{3 \times 3} \\ \mathbf{0}_{3 \times 3} & \mathbf{I}_H \end{bmatrix}, \quad \mathbf{D} = \begin{bmatrix} \mathbf{D}_1 & \mathbf{0}_{3 \times 3} \\ \mathbf{0}_{3 \times 3} & \mathbf{D}_2 \end{bmatrix}, \quad (8)$$

$$\mathbf{G}_1(\mathbf{q}) = \begin{bmatrix} mg\mathbf{R}_1^{-1}(\mathbf{q})\mathbf{e}_3 \\ \mathbf{0}_{3 \times 1} \end{bmatrix}, \quad (9)$$

$$\mathbf{C}_B(\boldsymbol{\zeta})\boldsymbol{\zeta} = \begin{bmatrix} \mathbf{0}_{3 \times 3} & \mathbf{v}^b \times m\boldsymbol{\omega} \\ \mathbf{v}^b \times m\mathbf{v}^b & \boldsymbol{\omega} \times \mathbf{I}_H \boldsymbol{\omega} \end{bmatrix} = \begin{bmatrix} \mathbf{0}_{3 \times 3} & \mathbf{C}_{B12}(\boldsymbol{\omega})\mathbf{v}^b \\ \mathbf{C}_{B21}(\mathbf{v}^b)\mathbf{v}^b & \mathbf{C}_{B2}(\boldsymbol{\omega})\boldsymbol{\omega} \end{bmatrix}. \quad (10)$$

and  $m$  is the mass of the aircraft.  $\mathbf{I}_H$  is the inertia of the aircraft,  $g$  is the acceleration due to gravity and the vector  $\mathbf{e}_3 = [0 \ 0 \ 1]^T$ . The relative velocity vector between the airfield in which the aircraft flies and the aircraft is given by:

$$\boldsymbol{\zeta}_r = \boldsymbol{\zeta} - \boldsymbol{\zeta}_a, \quad (11)$$

where:

$$\boldsymbol{\zeta}_a = \begin{bmatrix} \mathbf{v}_a^b \\ \mathbf{0}_{3 \times 1} \end{bmatrix}, \quad (12)$$

is the air current velocity vector. The force and moment vector from the loading effect of added mass and inertia, due to the aircraft moving through an airfield is defined as:

$$\begin{bmatrix} \mathbf{M}_{A1} & \mathbf{0}_{3 \times 3} \\ \mathbf{0}_{3 \times 3} & \mathbf{I}_A \end{bmatrix} \begin{bmatrix} \dot{\mathbf{v}}_r^b \\ \dot{\boldsymbol{\omega}} \end{bmatrix} + \begin{bmatrix} \mathbf{0}_{3 \times 3} & \mathbf{v}_r^b \times \mathbf{M}_{A1}\boldsymbol{\omega} \\ \mathbf{v}_r^b \times \mathbf{M}_{A1}\mathbf{v}_r^b & \boldsymbol{\omega} \times \mathbf{I}_A \boldsymbol{\omega} \end{bmatrix} = \begin{bmatrix} \mathbf{f}_r^b \\ \boldsymbol{\tau}_r \end{bmatrix} \quad (13)$$

which can be rewritten as:

$$\mathbf{M}_A \dot{\boldsymbol{\zeta}}_r + \mathbf{C}_A(\boldsymbol{\zeta}_r)\boldsymbol{\zeta}_r = \begin{bmatrix} \mathbf{f}_r^b \\ \boldsymbol{\tau}_r \end{bmatrix}, \quad (14)$$

is the load due to the air current velocity  $\mathbf{v}_c$ . Furthermore, we define  $\boldsymbol{\zeta}_a$ ,  $\mathbf{M}_A$  and  $\mathbf{C}_A(\boldsymbol{\zeta}_a)$  as:

$$\boldsymbol{\zeta}_a = \begin{bmatrix} \mathbf{v}_a^b \\ \mathbf{0}_{3 \times 1} \end{bmatrix}, \quad \mathbf{M}_A = \begin{bmatrix} \mathbf{M}_{A1} & \mathbf{0}_{3 \times 3} \\ \mathbf{0}_{3 \times 3} & \mathbf{I}_A \end{bmatrix},$$

$$\mathbf{C}_A(\boldsymbol{\zeta}_a)\boldsymbol{\zeta}_a = \begin{bmatrix} \mathbf{0}_{3 \times 3} & \mathbf{v}_a^b \times \mathbf{M}_{A1}\boldsymbol{\omega} \\ \mathbf{v}_a^b \times \mathbf{M}_{A1}\mathbf{v}_a^b & \boldsymbol{\omega} \times \mathbf{I}_A \boldsymbol{\omega} \end{bmatrix}$$

$$= \begin{bmatrix} \mathbf{0}_{3 \times 3} & \mathbf{C}_{A12}(\mathbf{v}_a^b)\boldsymbol{\omega} \\ \mathbf{C}_{A21}(\mathbf{v}_a^b)\mathbf{v}_a^b & \mathbf{C}_{A22}(\boldsymbol{\omega})\boldsymbol{\omega} \end{bmatrix}. \quad (15)$$

The wind force and moment vector  $\mathbf{f}_{Aero}$ ,  $\boldsymbol{\tau}_{Aero}$  due to the aircraft moving through a moving airfield is given by:

$$\begin{bmatrix} \mathbf{f}_{Aero} \\ \boldsymbol{\tau}_{Aero} \end{bmatrix} = \mathbf{g}_{\text{wind}} \gamma_{rv} V_{rv}^2, \quad (16)$$

where  $\mathbf{g}_{\text{wind}}$  is a vector depending on the air density  $\gamma_{rv}$ , wind coefficients, and frontal and lateral projected areas of the aircraft and  $V_{rv}$  is the relative wind speed to the aircraft. Considering that in practice airflow will comprise of both laminar and turbulent flow, these two components will be considered as deterministic and stochastic respectively. We can state:

$$\mathbf{v}_a^b = \bar{\mathbf{v}}_a^b + \tilde{\mathbf{v}}_a^b, \quad (17)$$

$$\boldsymbol{\zeta}_a = \bar{\boldsymbol{\zeta}}_a + \tilde{\boldsymbol{\zeta}}_a, \quad (18)$$

$$\mathbf{f}_{Aero} = \bar{\mathbf{f}}_{Aero} + \tilde{\mathbf{f}}_{Aero}, \quad (19)$$

$$\mathbf{f}_{Aero}^b = \bar{\mathbf{f}}_{Aero}^b + \tilde{\mathbf{f}}_{Aero}^b, \quad (20)$$

$$\mathbf{f}_{Aero} = \mathbf{R}_1(\mathbf{q})\mathbf{f}_{Aero}^b, \quad (21)$$

$$\boldsymbol{\tau}_{Aero} = \bar{\boldsymbol{\tau}}_{Aero} + \tilde{\boldsymbol{\tau}}_{Aero}. \quad (22)$$

Where  $\bar{\bullet}$  and  $\tilde{\bullet}$  denote the mean-value (deterministic) and zero-mean turbulent (stochastic) components of  $\bullet$  respectively. The deterministic components can be treated as unknown constants. The stochastic components are regarded as Gaussian random disturbances. By substituting equation (11) into the expressions for  $\mathbf{M}_A \dot{\zeta}_r$ ,  $\mathbf{D} \zeta_r$  and  $\mathbf{C}_A(\zeta_r) \zeta_r$  results in:

$$\mathbf{M}_A \dot{\zeta}_r = \mathbf{M}_A \dot{\zeta} - \mathbf{M}_A \dot{\zeta}_a, \quad (23)$$

$$\mathbf{D} \zeta_r = \mathbf{D} \zeta - \mathbf{D} \zeta_a, \quad (24)$$

$$\mathbf{C}_A(\zeta_r) \zeta_r = \mathbf{C}_A(\zeta) \zeta + \bar{\mathbf{C}}_A(\zeta_a) \zeta_a - (\mathbf{C}_A(\zeta) + \bar{\mathbf{C}}_A(\zeta)) \zeta_a, \quad (25)$$

$$\begin{aligned} \bar{\mathbf{C}}_A(\zeta) &= \begin{bmatrix} \mathbf{S}(\omega) \mathbf{M}_{A1} & \mathbf{0}_{3 \times 3} \\ \mathbf{S}(\mathbf{v}^b) \mathbf{M}_{A1} & \mathbf{S}(\omega) \mathbf{I}_A \end{bmatrix} \\ &= \begin{bmatrix} \bar{\mathbf{C}}_{A11}(\omega) & \bar{\mathbf{C}}_{A12} \\ \bar{\mathbf{C}}_{A21}(\mathbf{v}^b) & \bar{\mathbf{C}}_{A22}(\omega) \end{bmatrix}, \end{aligned} \quad (26)$$

In derivation of equation (24), we have used the property of the skew symmetric matrix, i.e.,  $\mathbf{S}(\mathbf{x})\mathbf{y} = -\mathbf{S}(\mathbf{y})\mathbf{x}$  for all  $\mathbf{x} \in \mathbb{R}^3$  and  $\mathbf{y} \in \mathbb{R}^3$ . Substituting equations (23), (24) and (25) into equation (4) yields:

$$\begin{aligned} \dot{\zeta} &= \mathbf{M}^{-1} \left( -\mathbf{D} \zeta - (\mathbf{C}_b(\zeta) + \mathbf{C}_A(\zeta)) \zeta - \mathbf{G}_1(\mathbf{q}) + \begin{bmatrix} \mathbf{f}^b \\ \boldsymbol{\tau} \end{bmatrix} \right) \\ &+ \mathbf{M}^{-1} \left( \mathbf{M}_A \dot{\zeta}_a + (\mathbf{C}_A(\zeta) + \bar{\mathbf{C}}_A(\zeta) + \mathbf{D}) \zeta_a - \bar{\mathbf{C}}_A(\zeta_a) \zeta_a \right. \\ &\quad \left. + \begin{bmatrix} \bar{\mathbf{f}}_{Aero}^b \\ \bar{\boldsymbol{\tau}}_{Aero} \end{bmatrix} \right). \end{aligned} \quad (27)$$

where  $\mathbf{M} = \mathbf{M}_b + \mathbf{M}_A$ . If we now alter equation (27), so that the linear position system is represented in the earth-fixed frame while leaving the angular position system in the body-fixed frame and combining with the first equations of (2) and equation (3) results in:

$$\begin{aligned} \dot{\eta}_1 &= \mathbf{v}_1, \\ \dot{\mathbf{v}}_1 &= -\mathbf{D}_1 \mathbf{v}_1 - g \mathbf{e}_3 + \mathbf{M}_1^{-1} (\mathbf{f} \mathbf{R}_1(\mathbf{q}) \mathbf{e}_3 + \bar{\mathbf{f}}_{Aero}), \\ \dot{\mathbf{q}} &= \mathbf{R}_2(\mathbf{q}) \boldsymbol{\omega}, \\ \dot{\boldsymbol{\omega}} &= (\mathbf{I}_A + \mathbf{I}_H)^{-1} \left( -\mathbf{D}_2 \boldsymbol{\omega} - \mathbf{C}_{A21}(\mathbf{v}^b) \mathbf{v}^b - \mathbf{C}_{B22}(\boldsymbol{\omega}) \boldsymbol{\omega} \right. \\ &\quad \left. - \mathbf{C}_{A22}(\boldsymbol{\omega}) \boldsymbol{\omega} + \boldsymbol{\tau} + \bar{\boldsymbol{\tau}}_{Aero} \right), \end{aligned} \quad (28)$$

where:

$$\mathbf{M}_1 = (m \mathbf{I}_{3 \times 3} + \mathbf{M}_{A1}). \quad (30)$$

Because  $\mathbf{v}_a^b = \bar{\mathbf{v}}_a^b + \tilde{\mathbf{v}}_a^b$  we have:

$$\mathbf{C}_A(\zeta_r) \zeta_r = \mathbf{C}_A(\bar{\zeta}_a) \bar{\zeta}_a - (\mathbf{C}_A(\bar{\zeta}_a) + \bar{\mathbf{C}}_A(\bar{\zeta}_a)) \tilde{\zeta}_a + \bar{\mathbf{C}}_A(\bar{\zeta}_a) \tilde{\zeta}_a, \quad (31)$$

substituting equation (31) into equation (27) gives:

$$\begin{aligned} d\zeta &= \mathbf{M}^{-1} \left( -\mathbf{D} \zeta - (\mathbf{C}_b(\zeta) + \mathbf{C}_A(\zeta)) \zeta - \mathbf{G}_1(\mathbf{q}) + \begin{bmatrix} \mathbf{f}^b \\ \boldsymbol{\tau} \end{bmatrix} \right) \\ &+ \mathbf{M}^{-1} \left( \mathbf{M}_A \dot{\zeta}_a + (\mathbf{C}_A(\zeta) + \bar{\mathbf{C}}_A(\zeta) + \mathbf{D}) \bar{\zeta}_a - \mathbf{C}_A(\bar{\zeta}_a) \bar{\zeta}_a \right) \\ &+ \mathbf{M}^{-1} \left( \mathbf{M}_A \dot{\zeta}_a + (\mathbf{C}_A(\zeta) + \bar{\mathbf{C}}_A(\zeta) + \mathbf{D}) \tilde{\zeta}_a - \mathbf{C}_A(\bar{\zeta}_a) \tilde{\zeta}_a \right) \\ &+ \mathbf{M}^{-1} \left( \mathbf{C}_A(\bar{\zeta}_a) \tilde{\zeta}_a - \bar{\mathbf{C}}_A(\bar{\zeta}_a) \tilde{\zeta}_a + \begin{bmatrix} \bar{\mathbf{f}}_{Aero}^b \\ \bar{\boldsymbol{\tau}}_{Aero} \end{bmatrix} + \begin{bmatrix} \tilde{\mathbf{f}}_{Aero}^b \\ \tilde{\boldsymbol{\tau}}_{Aero} \end{bmatrix} \right), \end{aligned} \quad (32)$$

If we now alter the above system of equations, so that the linear position system is represented in the earth inertial frame, while

leaving the angular position system in the body frame equation (32) becomes:

$$\begin{aligned} \dot{\eta}_1 &= \mathbf{v}_1, \\ d\mathbf{v}_1 &= \left( \mathbf{M}_1^{-1} (\mathbf{f} \mathbf{R}_1(\mathbf{q}) \mathbf{e}_3 + \bar{\mathbf{f}}_{Aero}) - \mathbf{D}_1 \mathbf{v}_1 - g \mathbf{e}_3 \right) dt + \mathbf{M}_1^{-1} \Delta_1(t) d\boldsymbol{w}_1, \quad (33) \\ \dot{\mathbf{q}} &= \mathbf{R}_2(\mathbf{q}) \boldsymbol{\omega}, \\ d\boldsymbol{\omega} &= (\mathbf{I}_A + \mathbf{I}_H)^{-1} \left( -\mathbf{D}_2 \boldsymbol{\omega} - \mathbf{C}_{B22}(\boldsymbol{\omega}) \boldsymbol{\omega} - \mathbf{C}_{A21}(\mathbf{v}^b) \mathbf{v}^b \right. \\ &\quad \left. - \mathbf{C}_{A22}(\boldsymbol{\omega}) \boldsymbol{\omega} + \boldsymbol{\tau} + \bar{\boldsymbol{\tau}}_{Aero} \right) dt \\ &+ (\mathbf{I}_A + \mathbf{I}_H)^{-1} \left( \mathbf{C}_{A21}(\mathbf{v}^b) + \mathbf{C}_{A22}(\boldsymbol{\omega}) + \bar{\mathbf{C}}_{A21}(\mathbf{v}^b) + \bar{\mathbf{C}}_{A22}(\boldsymbol{\omega}) \right. \\ &\quad \left. + \mathbf{D}_2 \right) \Delta_2(t) d\boldsymbol{w}_2 + (\mathbf{I}_A + \mathbf{I}_H)^{-1} \Delta_3(t) d\boldsymbol{w}_3, \quad (34) \end{aligned}$$

where  $\boldsymbol{w}_1$ ,  $\boldsymbol{w}_2$  and  $\boldsymbol{w}_3$  denote the 3-dimensional Wiener standard process vectors. The terms  $\bar{\mathbf{f}}_{Aero}$ ,  $\bar{\boldsymbol{\tau}}_{Aero}$  and  $\mathbf{C}_{A21}(\mathbf{v}^b) \mathbf{v}^b + \mathbf{C}_{A22}(\boldsymbol{\omega}) \boldsymbol{\omega}$  represent the mean value of forces and moments induced by wind gusts and aerodynamic loading due to travelling through an airfield. Moreover, the terms  $\Delta_1(t) \boldsymbol{w}_1$ ,  $(\mathbf{C}_{A21}(\mathbf{v}^b) + \mathbf{C}_{A22}(\boldsymbol{\omega}) + \bar{\mathbf{C}}_{A21}(\mathbf{v}^b) + \bar{\mathbf{C}}_{A22}(\boldsymbol{\omega}) + \mathbf{D}_2) \Delta_2(t) \boldsymbol{w}_2$  and  $\Delta_3(t) \boldsymbol{w}_3$ , where the dot denotes the normal time derivative, represents their stochastic components.

## Simulations

Using the model presented in the previous section, we will present a simulation of the aircraft being controlled by a combined one-step ahead backstepping and standard backstepping controller [18]. Furthermore, by incorporating weak and strong nonlinear Lyapunov functions it is possible to overcome difficulties caused by underactuation and Hessian terms. These Hessian terms are induced by the stochastic differentiation rule during the control design. To overcome the inherent underactuation of the aircraft, the roll and pitch angles of the aircraft are considered as immediate controls and are generated by the controller. A projection algorithm is introduced to design estimates of the deterministic components, and covariances of the stochastic components of the aerodynamic loads. To overcome difficulties associated with unmeasured linear velocities, output state feedback is used to estimate the quadrotors linear velocity. The aircraft's parameters are taken as  $m = 2.0$  kg,  $\mathbf{M}_{A1} = 0.1 \mathbf{I}_{3 \times 3}$  kg,  $\mathbf{I}_H = 10^{-3} \text{diag}(5, 5, 9)$  kg/m<sup>2</sup>,  $\mathbf{I}_A = 0.2 \mathbf{I}_H$  kg/m<sup>2</sup>,  $\mathbf{D}_1 = \text{diag}(0.25, 0.25, 0.125)$  kg/s<sup>2</sup>,  $\mathbf{D}_2 = 10^{-3} \text{diag}(2.5, 2.5, 0.03)$  kg/(sm)<sup>2</sup>,  $g = 9.81 \text{ms}^{-2}$ . The covariance matrices are taken as  $\Delta_1 = 0.1 \mathbf{I}_{3 \times 3}$ ,  $\Delta_2 = \mathbf{I}_{3 \times 3}$ ,  $\Delta_3 = 0.1 \mathbf{I}_{3 \times 3}$ . The mean values of environmental disturbances are taken as  $\bar{\mathbf{f}}(t) = \text{diag}(0.5, 0.5, 0.1)$  N,  $\bar{\boldsymbol{\tau}}(t) = \text{diag}(-1, -1, 0.1)$  Nm and  $\bar{\mathbf{v}}_a^b = [1, 1, 0.5]^T$ . The reference trajectories are taken as  $\boldsymbol{\eta}_{1d}(t) = [10 \cos(0.1t) - 20, 10 \sin(0.1t), 0.1t]^T$ , and  $\psi_a(t) = 0.01t$ . The initial states are taken as  $\boldsymbol{\eta}_1(t_0) = [10, 0, 0]^T$ ,  $\mathbf{v}_1(t_0) = [0, 0, 0]^T$ ,  $\mathbf{q} = [0, 0, 0]^T$  and  $\boldsymbol{\omega} = [0, 0, 0]^T$ . Excellent simulation results are plotted in Figure 2 and contrasted by Figure 3, which highlight the effects of ignoring turbulence. The position reference trajectory  $\boldsymbol{\eta}_{1d}$  and the position real trajectory  $\boldsymbol{\eta}_1$  are plotted in Figure 2 in all  $xyz$ -,  $xy$ -,  $xz$ -, and  $yz$  planes. The green curves denote the reference trajectories while the blue curves represent the real trajectories for the quadrotor. Contrasting the results of Figure 2 is Figure 3 which represents the quadrotor under a controller designed in the same manner, but does not take into account the turbulent dynamics. Moreover, it is clear that turbulent aerodynamic loads have an adverse effect on the performance of the quadrotor which is of concern considering the popular use of quadrotors in our current society.

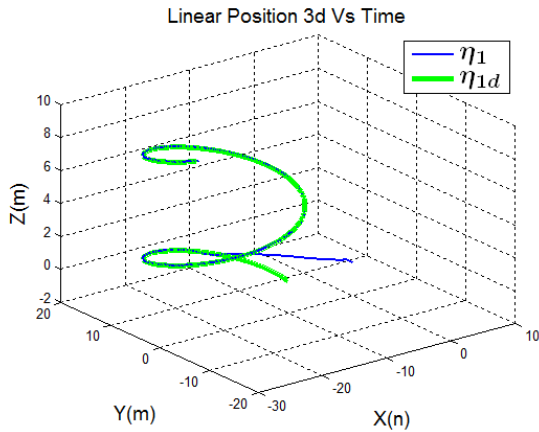


Figure 2: Quadrotor helicopter with turbulent disturbance compensation.

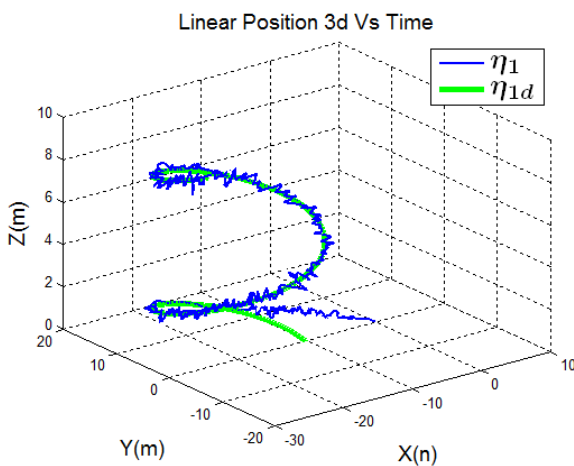


Figure 3: Quadrotor helicopter without turbulent disturbance compensation.

## Conclusions

A detailed model of a quadrotor aircraft in three-dimensional space exposed to environmental disturbances resulting from both laminar and turbulent airflow has been presented. The effects on controlling the quadrotor under these conditions has been demonstrated. Simulation results show that by not taking into account the turbulent aerodynamic loads that a quadrotor experiences during flight has an adverse effect on the aircrafts performance. However, when these aerodynamic loads are taken into account the aircraft performs notably well as it is able to compensate for these disturbances. The use of SDEs help to model the behaviour of the chaotic aerodynamic loads resulting from turbulence and, is therefore able to be compensated for when designing a controller.

## Acknowledgments

The author would like to express his sincere gratitude to the Associate Editor and the reviewers for their time taken reviewing this paper.

## References

- [1] K. D. Do and J. Pan, *Control of Ships and Underwater Vehicles: Design for Underactuated and Nonlinear Marine Systems*, London: Springer, 2009.
- [2] S. M. Joshi, A. G. Kelkar and J. T.-Y. Wen, "Robust attitude stabilization of spacecraft using nonlinear quaternion feedback," *IEEE Transactions on Automatic Control*, vol. 40, no. 10, p. 1800–1803, 1995.

- [3] A. Tayebi and S. McGilvray, "Attitude stabilization of a VTOL quadrotor aircraft," *IEEE Transactions on Control Systems Technology*, vol. 14, no. 3, pp. 562-571, 2006.
- [4] P. Castillo, A. Dzul and R. Lozano, "Real-time stabilization and tracking of a four-rotor mini rotorcraft," *IEEE Transactions on Control Systems Technology*, vol. 12, no. 4, p. 510–516, 2004.
- [5] T. Madani and A. Benallegue, "Control of a quadrotor mini-helicopter via full state backstepping technique," in *Proceedings of the 45th IEEE Conference on Decision & Control*, San Diego, 2006.
- [6] Z. Zuo, "Trajectory tracking control design with command-filtered compensation for a quadrotor," *IET Control Theory and Applications*, vol. 4, no. 11, pp. 1515-1520, 2010.
- [7] A. Abdessameud and A. Tayebi, "Global trajectory tracking control of VTOL-UAVs without linear velocity measurements," *Automatica*, vol. 46, no. 6, pp. 1053-1059, 2010.
- [8] A. Roberts and A. Tayebi, "Adaptive position tracking of VTOL UAVs," *IEEE Transactions on Robotics*, vol. 27, no. 1, pp. 129-142, 2011.
- [9] Y. C. Choi and H. S. Ahn, "Nonlinear control of quadrotor for point tracking: Actual implementation and experimental tests," *IEEE/ASME Transactions on Mechatronics*, vol. 20, no. 3, pp. 1179-1192, 2015.
- [10] X. Ding and Y. Yu, "Motion planning and stabilization control of a multipropeller multifunction aerial robot," *IEEE/ASME Transactions on Mechatronics*, vol. 18, no. 3, pp. 645-656, 2013.
- [11] D. Lee, A. Franchi, H. I. Son, C. Ha, H. H. Bulthoff and P. R. Giordano, "Semiautonomous haptic teleoperation control architecture of multiple unmanned aerial vehicles," *IEEE/ASME Transactions on Mechatronics*, vol. 18, no. 4, p. 1334–1345, 2013.
- [12] M. Xin, Y. Xu and R. Hopkins, "Trajectory control of miniature helicopters using a unified nonlinear optimal control technique," *Journal of Dynamic Systems, Measurement, and Control*, vol. 13, no. 6, p. 061001–1:061001–14, 2011.
- [13] K. D. Do and J. Paxman, "Global Tracking Control of Quadrotor VTOL Aircraft in Three Dimensional Space," *Control Conference (AUCC), 2013 3rd Australian*, p. 26–33, 2013.
- [14] A. Zavala-Rio, I. Fantoni and R. Lozano, "Global stabilization of a pvtol aircraft model with bounded inputs," *International Journal of Control*, vol. 76, no. 18, pp. 1833-1844, 2003.
- [15] P. Castillo, A. Dzul and R. Lozano, "Real-time stabilization and tracking of a four-rotor mini rotorcraft," *IEEE Transactions on Control Systems Technology*, vol. 12, no. 4, pp. 510-516, 2004.
- [16] A. Ailon, "Simple tracking controllers for autonomous VTOL aircraft with bounded inputs," *IEEE Transactions on Automatic Control*, vol. 55, no. 3, p. 737–743, 2010.
- [17] A. Zavala-Rio, I. Fantoni and G. Sanahuja, "Finite-time observer-based output-feedback control for the global stabilisation of the pvtol aircraft with bounded inputs," *International Journal of Systems Science*, vol. 47, no. 7, p. 1543–1562, 2014.
- [18] A. R. Teel, "Global stabilization and restricted tracking for multiple integrators with bounded control," *Systems and Control Letters*, vol. 18, no. 3, p. 165–171, 1992.

